Internal resonance between in-plane and out-of-plane modes of vibration of inclined cables subjected to vertical support excitation.

Vassil Tzanov, Maria Rosaria Marsico, David Wagg, Bernd Krauskopf, Simon Neild, John Macdonald
Faculty of Engineering, University of Bristol, Queen's Building, Bristol, BS8 1TR, United Kingdom
email: V.Tzanov@bristol.ac.uk, m.r.marsico@bristol.ac.uk, David.Wagg@bristol.ac.uk, B.Krauskopf@bristol.ac.uk, Simon.Neild@bristol.ac.uk, john.macdonald@bristol.ac.uk

ABSTRACT: Inclined cables are important structural elements of cable-stayed bridges. When the bridge deck oscillates, large amplitude cable vibrations can arise in various modes as a result of the low cable damping, parametric excitation or non-linear modal coupling. The resulting vibrations are undesirable and potentially damaging to the long-term performance of the bridge. The phenomena can be modelled considering internal resonances between in-plane and out-of-plane modes of vibration of the cable. Here they have been studied using a four-mode model that represents the response of an inclined cable vertically excited at the lower end (i.e. from the deck) with a frequency that is close to the natural frequency of the second cable mode in each plane and twice the frequency of the first mode in each plane. The modal equations of the model are investigated using the software package AUTO for the numerical continuation of solutions of a system of ODEs. This allows the identification of the important solution branches in the cable model responsible for unwanted vibration behaviour. The result of our analysis is that we identify amplitudes of excitation above which modes other than the directly excited mode (the second in-plane mode) start contributing to the response of the cable. In addition, we show that the response amplitudes in these additional modes is of similar magnitude to the amplitudes in the directly excited mode, which could be considered an issue in the design of cable-stayed bridges. In summary, by using a numerical continuation technique we predict when the response of the cable will change from a single in-plane mode to coupled responses in two or more modes, in-plane or in both planes, and the modal amplitudes involved in these coupled responses.

KEY WORDS: Cable vibration; Internal resonance; Sway motion; Modal interaction; Bifurcation analysis.

1 INTRODUCTION

The inclined cables of cable-stayed bridges are typically lightly damped. When the bridge deck oscillates (typically from wind or traffic excitation) it provides a support motion input to the cable. This type of excitation can lead to large amplitude vibrations of the cable [1]. A case of particular interest is when the deck motion is at two times a natural frequency of the cable, which can lead to large amplitude parametrically excited vibrations. This phenomenon was studied in [2] by using a nonlinear Mathieu-type equation to model the parametric resonance [3]. However, since the cables are taut, the natural frequencies are almost at pure harmonics of the fundamental mode, so two times one natural frequency closely coincides with another mode, which is directly excited by the same input [4], [5]. Furthermore internal resonance occurs between the in-plane and out-of-plane modes, so non-linear coupling leads to out-of-plane responses for in-plane excitation. The deck motions are generally larger at lower frequencies, so the most significant responses often occur for deck motions around the second natural frequency of the cable, where small deck inputs can cause large responses in the first and second modes in both planes.

In this paper the Warnitchai equations [6] (see also [7] for a detailed derivation) are used to model the vibration of the cable. It is assumed that the longitudinal vibrations of the cable can be neglected, so that the planes of interest are vertical (in-plane) and sway (out-of-plane).

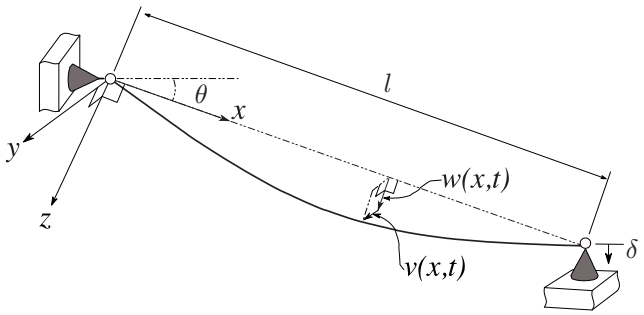

Figure 1. Schematic representation of an inclined cable with vertical input motion at the lower attachement point.

Four modes are included in the model, two in-plane and two out-of-plane, which enables the important low frequency dynamic behaviour to be modelled [8], [9]. The Warnitchai equations are scaled and averaged using the same procedure as previously presented in [4], [5]. Then a bifurcation study is carried out by means of numerical continuation [10] with the software package AUTO [11]. In this way, a series of bifurcation diagrams are produced for different values of the detuning parameter of the excitation frequency (with respect to the second in-plane natural frequency) with the aim of studying the behaviour of modal amplitudes of the response of the cable close to the resonance frequency. The result is a general picture of the stable and unstable branches and all interactions between the bifurcation

$$
\begin{aligned}
y'_{1c} &= \left(\frac{W_{12}z_{1c}z_{1s}}{16\omega_1} - \xi\omega_1\right)y_{1c} - \left(\mu\omega_1 + \frac{N_1\Delta}{4\omega_1} - \frac{W_{12}}{32\omega_1}\left(C_1 - 2z_{1c}^2\right)\right)y_{1s},\\
y'_{1s} &= \left(\mu\omega_1 - \frac{N_1\Delta}{4\omega_1} - \frac{W_{12}}{32\omega_1}\left(C_1 - 2z_{1s}^2\right)\right)y_{1c} - \left(\xi\omega_1 + \frac{W_{12}z_{1c}z_{1s}}{16\omega_1}\right)y_{1s},\\
y'_{2c} &= \left(\frac{W_{12}z_{2c}z_{2s}}{2\omega_1} - 2\xi\omega_1\right)y_{2c} - \left(2\mu\omega_1 - \frac{W_{12}}{8\omega_1}\left(C_2 - 4z_{2c}^2\right)\right)y_{2s},\\
y'_{2s} &= \left(2\mu\omega_1 - \frac{W_{12}}{8\omega_1}\left(C_2 - 4z_{2s}^2\right)\right)y_{2c} - \left(2\xi\omega_1 + \frac{W_{12}z_{2c}z_{2s}}{2\omega_1}\right)y_{2s},\\
z'_{1c} &= \left(\frac{W_{12}y_{1c}y_{1s}}{16\omega_1} - \xi\omega_1\right)z_{1c} - \left((\mu-\kappa)\omega_1 + \frac{N_1\Delta}{4\omega_1} - \frac{W_{12}}{32\omega_1}\left(C_1 - 2y_{1c}^2\right)\right)z_{1s},\\
z'_{1s} &= \left((\mu-\kappa)\omega_1 - \frac{N_1\Delta}{4\omega_1} - \frac{W_{12}}{32\omega_1}\left(C_1 - 2y_{1s}^2\right)\right)z_{1c} - \left(\xi\omega_1 + \frac{W_{12}y_{1c}y_{1s}}{16\omega_1}\right)z_{1s},\\
z'_{2c} &= \left(\frac{W_{12}y_{2c}y_{2s}}{2\omega_1} - 2\xi\omega_1\right)z_{2c} - \left(2\mu\omega_1 - \frac{W_{12}}{8\omega_1}\left(C_2 - 4y_{2c}^2\right)\right)z_{2s},\\
z'_{2s} &= \left(2\mu\omega_1 - \frac{W_{12}}{8\omega_1}\left(C_2 - 4y_{2s}^2\right)\right)z_{2c} - \left(2\xi\omega_1 + \frac{W_{12}y_{2c}y_{2s}}{2\omega_1}\right)z_{2s} - B\Delta\omega_1.
\end{aligned}
\tag{1}
$$

loci curves in the space defined by the norm of the solutions and both main parameters (input amplitude and frequency). In addition, one of these solution branches is discussed in more detail regarding the response amplitudes in all modes that our model includes.

The remainder of this paper is structured as follows. In Section 2 the equations of motion for the inclined cable model are presented as derived via scaling and first-order averaging. Section 3 describes the bifurcation study and numerical continuation analysis. Conclusions are drawn in Section 4.

2 MODAL AMPLITUDE EQUATIONS

In this paper we use a mathematical model of an inclined cable, see Figure 1, which is excited vertically at the bottom anchorage with amplitude Δ and angular frequency Ω where its upper anchorage stays in the rest position [4]. Our model is based on the Warnitchai equations used in [4], [5], [6], [7]. In the Warnitchai derivation, the out-of-plane and in-plane modal response of the cable are given by

$$
\begin{aligned}
v(x,t) &= \textstyle\sum_{n=1}^{\infty}\phi_n(x)y_n(t),\\
w(x,t) &= \textstyle\sum_{n=1}^{\infty}\psi_n(x)z_n(t),
\end{aligned}
$$

respectively, where $x \in [0,\ell]$, ℓ is the support separation distance, the spatial functions $\phi(x)$ and $\psi(x)$ are the out-of-plane and in-plane linear modes of a cable with fixed ends, and $y_n(t)$ and $z_n(t)$ their corresponding time-dependent generalised coordinates. The mode shapes for the out-of-plane and even in-plane modes of the linearised system are assumed to be:

$$
\begin{aligned}
\phi_n &= \sin\left(n\pi\frac{x}{\ell}\right) \qquad \text{for} \quad n = 1,2,3,\ldots,\\
\psi_n &= \sin\left(n\pi\frac{x}{\ell}\right) \qquad \text{for} \quad n = 2,4,6,\ldots.
\end{aligned}
$$

For the odd in-plane modes the mode shapes are more complex; however, as is discussed in [7], for taut cables they may be approximated by sine functions of the same form as the out-of-plane modes. To derive the time-dependent generalised coordinates we can use the non-autonomous system with eight ODEs, see [5] where the original Warnitchai equations of motion of the cable are scaled and averaged to became Equations (1). Here, $C_1 = 3M_1 + 8M_2$, $C_2 = M_1 + 6M_2$, where $M_1 = y_{1c}^2 + y_{1s}^2 + z_{1c}^2 + z_{1s}^2$ and $M_2 = y_{2c}^2 + y_{2s}^2 + z_{2c}^2 + z_{2s}^2$. Furthermore, $\kappa = k_1/2$, $W_{nk} = \nu_{nk}/m$, $N_n = 2\eta_n \sin\theta/m$, $B = \zeta_2\cos\theta/m$ and $\delta = \Delta\cos(\Omega t)$; numerical values for the cable parameters are given in Table 1 and Table 2 based on the scaled-model cable tested in [5]. In the expressions for W_{nk}, N_n and B:

Table 1. Dimensional cable parameters

N_1 [Hz^2/m]	W_{12} [1/(s.m)^2]	ω_1 [rad/s]
1.04×10^{-4}	5.19×10^{-4}	20.4852

Table 2. Nondimensional cable parameters.

B	ξ	κ
0.2939	0.002	0.0234

$m = \rho A\ell/2$ is the modal mass of the cable (for all modes), θ is the angle between the cable chord and the horizontal plane, σ_s is the static stress, λ^2 is Irvine's parameter, A is the cross sectional area, ρ is the density, g is gravity and E is Young's modulus;

ω_n is the n-th natural frequency of the cable. The equivalent modulus of the cable E_q, the distributed weight perpendicular to the cable chord γ, and the parameters $\nu_{nk}, \eta_n, \zeta_n$ are given by:

$$E_q = \frac{1}{1+\lambda^2/12}E, \quad \lambda^2 = \frac{E}{\sigma_s}\left(\frac{\gamma\ell}{\sigma_s}\right)^2, \quad \gamma = \rho g\cos\theta,$$
$$\nu_{nk} = \frac{EA\pi^4 n^2 k^2}{8\ell^3}, \quad \eta_n = \frac{E_q A\pi^2 n^2}{4\ell^2}, \quad \zeta_n = \frac{2m}{n\pi}.$$

The out-of-plane and in-plane natural frequencies, ω_{yn} and ω_{zn} respectively, are given by

$$\omega_{yn} = \frac{n\pi}{\ell}\sqrt{\frac{\sigma_s}{\rho}}, \quad \omega_{zn} = \frac{n\pi}{\ell}\sqrt{\frac{\sigma_s}{\rho}(1+k_n)},$$

where k_n is due to the effect of sag and is given by

$$k_n = \left(\frac{2\lambda^2}{\pi^4 n^4}\right)\left(1+(-1)^{n+1}\right)^2.$$

The vibration response of the cable presented by Equations (1) can be expressed by the amplitude contributions of two in-plane and two out-of-plane modal amplitudes:

- $Z_2 = \sqrt{z_{2c}^2 + z_{2s}^2}$ for the second in-plane modal amplitude;
- $Z_1 = \sqrt{z_{1c}^2 + z_{1s}^2}$ for the first in-plane modal amplitude;
- $Y_2 = \sqrt{y_{2c}^2 + y_{2s}^2}$ for the second out-of-plane modal amplitude;
- $Y_1 = \sqrt{y_{1c}^2 + y_{1s}^2}$ for the first out-of-plane modal amplitude.

The amplitude of excitation Δ and the detuning $\mu = \Omega/\omega_2 - 1$ between the frequency of the actuator and the second natural frequency of the cable are the main parameters of Equations (1). The non-dimensional values that are used when we vary the parameters of the system are Δ/L and μ, where $L = 5.4m$ is the untensioned cable length measured from the top of the cable to its bottom, and $L \approx \ell$. The norm $||N|| = \sqrt{Z_2^2 + Z_1^2 + Y_2^2 + Y_1^2}/L$ of the solutions of Equations (1) is a function of Δ/L and μ, which we use to measure the changes of the behaviour of the cable response.

3 BIFURCATION STUDY

Our system in the form of ODEs (1) can be examined with the continuation software AUTO [10], [11]. In our study we follow the stable solutions of Equations (1) from zero forcing amplitude, hence zero response amplitude, and different values of forcing frequency close to the second natural frequency of the cable. Therefore we fix the forcing frequency and vary the excitation amplitude. This leads to increasing amplitude of the response of the cable. Because the averaging technique is based on modal decomposition, we are analysing how the modal amplitudes of the response change as the excitation amplitude increases from zero to positive values. In the resulting bifurcation diagrams [12], [13], stable and unstable solution branches can be identified. Since the stable solutions define the possible modes of behaviour of the physical cable system we can calculate each modal contribution to the overall vibration response. By combining multiple continuations of this type, each one for a different frequency close to 2:1 resonance, we obtain a set of solution curves of Equations (1).

3.1 *Stability boundaries in* $(\Delta/L, \mu, ||N||)$*-space*

Series of solution curves of Equations (1) of the following types $(Z_2 \neq 0, Z_1 = Y_2 = Y_1 = 0)$ for $(\Delta/L, \mu) \in [0, 6.2\times 10^{-3}] \times [-0.03, 0.07]$ give us a set of solution branches Γ in $(\Delta/L, \mu, ||N||)$-space, see Figure 2. The solution curve for $\mu = 0.01$ is shown colourless to identify the intersection of Γ with the $(\Delta/L, 0.01, ||N||)$-plane; it is the bold white curve that is labelled l_1. Later in this paper, the bifurcation curve l_1 will be explained in detail. Γ could be constructed if we derive the equation of the surface that contains it by numerically solving only the last couple of equations responsible for the Z_2-mode [5], the directly excited mode, while taking into account that all other modes have no contribution.

In Figure 2 dark grey represents the stable parts of the solution curves and light the unstable ones. The curves B_{Y_1}, B_{Y_2}, B_{Z_1} and F_{Z_2}, drawn black, are respectively the loci of the branch points of Y_1, Y_2 and Z_1-modal amplitudes and the fold points of the Z_2-modal amplitudes. When it forms a boundary between dark and light parts then the respective bifurcation concerns a stable solution. This is the case for B_{Y_1} on the left of the crossing point N, for B_{Y_2} between the crossing points N and M, for F_{Z_2} between the crossing points M and the crossing point K, and for B_{Z_1} between crossing point K and the right end of the region of μ. Otherwise, the respective bifurcation concerns an unstable solution. In Figure 2 we can see the interactions of the bifurcation curves at crossing points N, M, K and the cusp point C [12], [13] therefore, we have a general picture of how the dynamics of the cable changes when we vary μ or Δ/L by the already shown stability boundaries of the pure Z_2-modal amplitudes response region, the dark grey region of Γ in Figure 2.

The approximate coordinates of the points N, M, C and K in $(\Delta/L, \mu, ||N||)$-space, for the chosen cable parameters, are
$(0.8\times 10^{-4}, 0.0036, 2.4\times 10^{-3})$ for N,
$(0.9\times 10^{-4}, 0.062, 6.8\times 10^{-3})$ for M,
$(0.2\times 10^{-4}, 0.0035, 1.3\times 10^{-3})$ for C, and
$(2.2\times 10^{-4}, 0.021, 2.3\times 10^{-3})$ for K.
Hence if the B_{Y_1}-curve is crossed for $\mu \in [-0.03, 0.0036]$ as Δ/L is increased for a fixed μ, we would experience out-of-plane motion due to the presence of stable branches that include the Y_1 mode. The parts B_{Y_1} and F_{Z_2} which concern stable solutions, approach each other, and they enclose a region that corresponds to pure Z_2-modal amplitude. This region is crossed by the B_{Z_1}-curve. There are two crossings, one is between B_{Y_1} and B_{Z_1} and another is between F_{Z_2} and B_{Z_1} but, because they are close enough, we only indicate the point M in between to denote these crossings. Thus if the B_{Y_2}-curve is crossed for $\mu \in [0.0036, 0.062]$, that is, between points N and M, as Δ/L is increased for a fixed μ, we would experience out-of-plane motion due to presence of stable branches that include Y_2 mode. If the F_{Z_2}-curve is crossed for $\mu \in [0.0035, 0.0062]$, that is, between points C and M, as Δ/L is decreased for a fixed μ, we would experience a hysteresis jump down to another pure Z_2-modal amplitudes that correspond to solutions with lower norm $||N||$. If the F_{Z_2}-curve is crossed for $\mu \in [0.0035, 0.021]$, that is, between points C and K, as Δ/L is increased for a fixed μ, we would experience out-of-plane motion due to a hysteresis

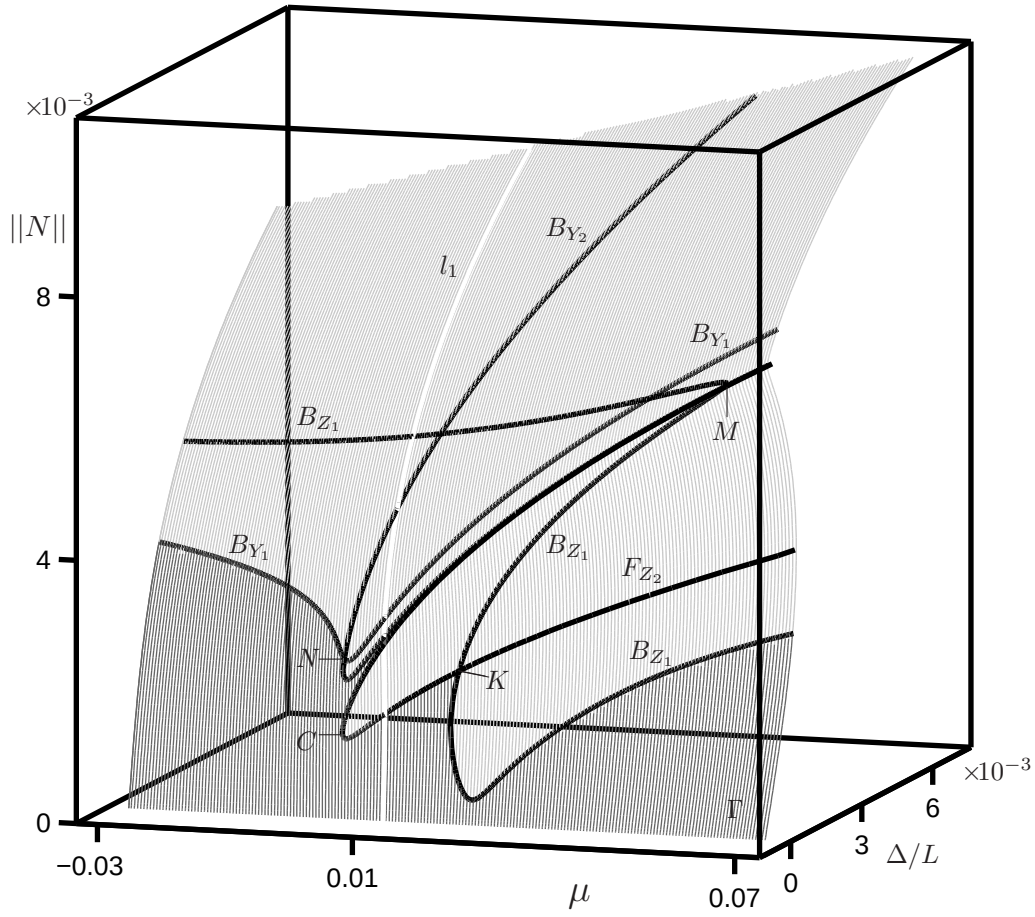

Figure 2. The set of solution branches Γ in $(\Delta/L, \mu, ||N||)$-space, obtained by a series of continuations of Equation (1); its intersection with the $(\Delta/L, ||N||)$-plane for $\mu = 0.01$ is the bold white curve denoted l_1. Solution branches including a pure Z_2-mode are gray; stable regions are shown dark and unstable region light. Bifurcation curves B_{Y_1}, B_{Y_2}, B_{Z_1} and F_{Z_2}, are black, and the bifurcation points C, K, N and M are labeled.

jump to another stable solution branches that include Y_1 and Y_2 modes. As an example of this case we will discuss in details how the cable response changes when Δ/L is increased for fixed $\mu = 0.01$. Finally if the B_{Z_1}-curve is crossed for $\mu \geq 0.021$ as Δ/L is increased for a fixed μ, where B_{Z_1} concerns stable solution, we would experience vibration amplitudes that are not only in a pure Z_2-mode. In this case our theoretical study is not complete yet, the possible presence of stable limit cycles in this region makes the prediction of the dynamics beyond the Z_1 branch point curve hard to achieve. As can be seen in [5], most of the stability boundaries of Z_2-amplitude that are shown in Figure 2 are experimentally confirmed.

3.2 One-parameter bifurcation diagram

The set Γ of solutions in the $(\Delta/L, \mu, ||N||)$-space shown in Fig. 2 features four bifurcation curves. As we explained, these curves may give rise to additional branches of stable solutions or to some kind of hysteresis jump to other branches of stable solutions. To become familiar with one of these situations we pick the value $\mu = 0.01$ and perform a detailed continuation analysis by variation of the amplitude of excitation $\Delta/L \in [0, 7 \times 10^{-4}]$. Thus, Figure 3 presents the one-parameter bifurcation diagram of Equations (1) for fixed $\mu = 0.01$; it shows the properties of the solution branches $l_1 \in \Gamma_1$, l_2, l_3 and l_4, and how their stable (denoted by black) and unstable (denoted by grey) parts meet in bifurcation points. The bifurcation points that lie on l_1 also lie on Γ so they are the crossing points between l_1 and the bifurcation curves shown in Figure 2. More precisely, branch point bifurcations $B_1, B_3 \in B_{Y_2}$ and $B_2 \in B_{Y_1}$ are denoted by ■. Fold bifurcation points $F_1, F_2 \in F_{Z_2}$ are denoted by ●.

The continuation starts at zero amplitude and, as the excitation increases, we follow l_1 on which only the Z_2-amplitudes exist. Then at Δ/L approximately 0.74×10^{-4} a fold bifurcation point F_1 appears. The curve l_1 loses stability at F_1 and becomes unstable until it reaches a second bifurcation point F_2 at $\Delta/L \approx 0.37 \times 10^{-4}$. There it becomes stable again for a very small interval, see Figure 4 (enlarged view of Figure 3), until a branch point B_1 for $\Delta/L \approx 0.4 \times 10^{-4}$. Beyond the point B_1, l_1 stays unstable to the end of the region of interest of Δ/L. According to the instability of l_1 beyond F_1, if we increase Δ/L above 0.74×10^{-4}, a transition to another stable solution branch l_4 takes place. On l_4 the modal amplitudes Z_2, Y_1, and Y_2 are

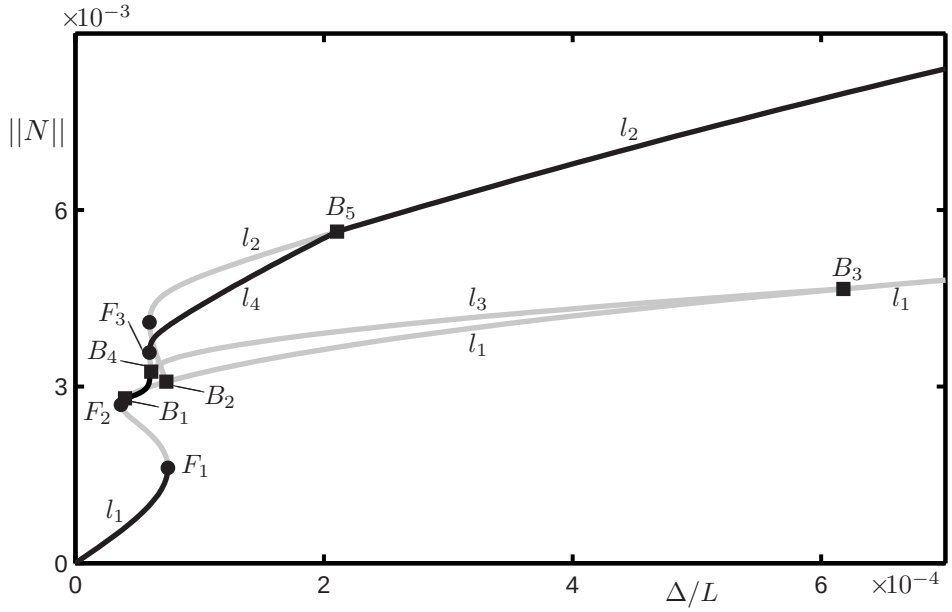

Figure 3. One-parameter bifurcation diagram of Equation (1) for $\mu = 0.01$, showing solution branches represented by their norm $||N|| = \sqrt{Z_2^2 + Z_1^2 + Y_2^2 + Y_1^2}/L$ for $\Delta/L \in [0, 7\times10^{-4}]$. The stable parts of the solution branches l_1–l_4 (black curves) are connected via their unstable parts (grey curves), which meet at bifurcation points. Specifically, $B_1 - B_5$ are branch points (denoted by ■) and $F_1 - F_3$ are fold points (denoted by ●).

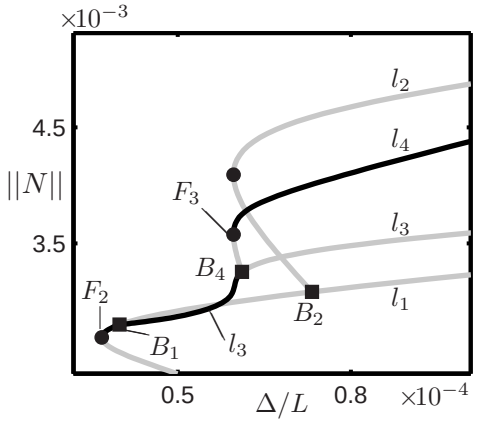

Figure 4. Scaled view of Figure 3, we look in the domain $(\Delta/L, ||N||) \in [0.3\times10^{-4}, 1\times10^{-4}] \times [2.3\times10^{-3}, 5.3\times10^{-3}]$ where we can distinguish how F_2 and B_1 are separated by a stable part of the l_1 solution branch, and the connections between the $l_1 - l_4$ branches.

non-zero, hence for Δ/L above 0.74×10^{-4}, strong out-of-plane amplitudes start contributing to the response of the cable. If we further increase Δ/L we will reach the branch point B_5 at $\Delta/L \approx 2.1\times10^{-4}$ that connects l_4 to the stable part of l_2 on which Y_1 and Z_2 amplitudes exist. Until the end of the region of continuation, l_2 remains stable and Y_1 is the only modal amplitude apart from Z_2 that contributes to the overall response of the cable. Here we have to explain how we found the stable part of l_2 and l_4, which are significant to our study because they give us the information on the dynamics of the cable past the point F_1 where we find an out-of-plane response. From the branch point B_1, see Figure 4, we start to compute solution curve l_3, which represents the Y_2 contributions to the cable response. In the beginning of this curve between B_1 and B_4, there exists a region where l_3 is stable. Beyond the bifurcation point B_4 at $\Delta/L \approx 0.61\times10^{-4}$, l_3 becomes unstable. It joins again l_1 at $\Delta/L \approx 6.2\times10^{-4}$. The point B_3 where l_3 joins l_1 again can be seen in Figure 2 as the intersection between the B_{Y_2} branch point curve and l_1. At $\Delta/L \approx 0.61\times10^{-4}$ there is a branch point B_4 on l_3, this branch point is the place where l_3 joins l_4, which is the solution curve on which the modal amplitudes Z_2, Y_1 and Y_2 exist. Until the fold point F_3 at $\Delta/L \approx 0.6\times10^{-4}$ l_4 is unstable; beyond this point the stable part of l_4 begins and it becomes physically observable as the solution branch that is responsible for the out-of-plane cable response that arises when Δ/L becomes larger than 0.74×10^{-4}, beyond the F_1 fold point. The onset of a contribution of the Y_1-amplitude to the Z_2-amplitude, i.e. the solution curve l_2 on which we remain for values of Δ/L higher than 2.1×10^{-4}, beyond branch point B_5 in Figure 3, goes back to the branch point B_2 on l_1 at $\Delta/L \approx 0.73\times10^{-4}$, see Figure 4. Between B_2 and B_5, the branch l_2 is unstable and does not effect the response of the cable.

The stable parts of the solution branches l_1, l_2, l_3, and l_4 are shown in Figures 5(a), (b), and (c) in order to show how the Z_2, Y_1, and Y_2-amplitudes contribute to the overall response of the cable for $\mu = 0.01$. Figure 5(a) shows that the Z_2-amplitude contributes to all the stable branches l_1 to l_4. The only modal amplitude that is involved in l_1 is the Z_2-amplitude; note that in Figures 5(b) and (c) l_1 is shown as zero response. Then, if Δ/L becomes larger than 0.74×10^{-4}, we jump from the point F_1 and the cable response vibrates with out-of-plane contributions from the Y_1-amplitude and from the Y_2-amplitude. As can be seen in Figures 5(b) and (c), l_4 appears as a non-zero curve. At B_5, l_4 joins l_2, which is the point where the Y_2-amplitude disappears and the cable response shows (Z_2, Y_1)-amplitudes only, until the end of the region of continuation of Δ/L. The contribution

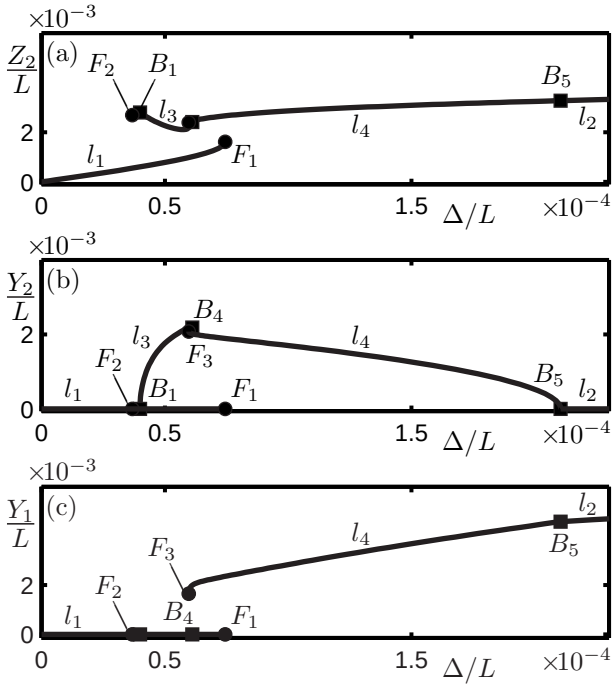

Figure 5. Modal amplitude contributions to the stable branches $l_1 - l_4$ for $\mu = 0.01$ from Figures 3 and 4, showing the contributions of (a) Z_2, (b) Y_2, and (c) Y_1 modes.

of the Z_2-amplitude and of the Y_2-amplitude to l_3, shown in Figure 5(a),(b), begins at the branch point B_1 and ends at the branch point B_4. The point B_1 lies on the small stable part of l_1, preceded by the unstable one beyond the fold point F_1, see Figures 3 and 4. Hence due to the unstable part of l_1 between F_1 and F_2, where Δ/L decreases, in Figure 5(a),(b) and (c), the points F_2 and B_1 come before F_1. Also, because the stable parts of both l_1 and l_3 appear as zero solutions in Figure 5(c), they overlap each other. It is important to note that the amplitudes at vibration modes Y_1 and Y_2 on solution branch l_4, and Y_1 on l_2 are both compatible with the amplitude of the directly excited mode Z_2.

4 CONCLUSIONS

In this paper we presented a theoretical study of the nonlinear vibration amplitudes of an inclined cable that is excited at its lower attachment point. Our analysis of the response in pure Z_2-modal amplitudes produced a set of solution curves that present the Z_2 vibration amplitude and the bifurcation curves as functions of the frequency and amplitude of the end displacement. In this way, bifurcation curves were presented without intersections, even though they may intersect and overlap when shown in the $(\Delta/L, \mu)$ parameters plane. A detailed bifurcation analysis for $\mu = 0.01$, a value of the detuning parameter close to the resonant frequency, was performed. Stable branches were identified and the modal amplitude contributions to those branches was shown. Overall, the continuation analysis results in an informative representation of the behaviour of the cable system in a region where the dynamics are extremely sensitive to changes of its driving parameters.

ACKNOWLEDGMENTS

The authors would like to acknowage the support from the Engineering and Physical Sciences Research Council (EPSRC) of the research of Dr. M.R.Marsico and V.Tzanov under grant EP/F030711/1

REFERENCES

[1] N. Srinil, G. Rega, S. Chucheepsakul, Three-dimensional non-linear coupling and dynamic tension in the large-amplitude free vibrations of arbitrarily sagged cables. *Journal of Sound & Vibration*, 269(3-5) (2004) 823–852.

[2] J. L. Lilien, A. P. Pinto Da Costa, Vibration amplitudes caused by parametric excitation of cable stayed structures. *Journal Sound & Vibration* 174 (1994) 69–90.

[3] T. Bakri, R. Nabergoj, A. Tonel, F. Verhulst, Parametric excitation in non-linear dynamics. *International Journal Non-linear Mechanics*, 39 (2004) 311–329.

[4] A. Gonzalez-Buelga, S.A. Neild, D.J. Wagg, J.H.G. Macdonald, Modal stability of inclined cables subjected to vertical support excitation. *Journal of Sound & Vibration*, 318 (2008) 565–579.

[5] J.H.G. Macdonald, M.S. Dietz, S.A. Neild, A. Gonzalez-Buelga, A.J. Crewe, D.J. Wagg, Generalised modal stability of inclined cables subjected to support excitations. *Journal of Sound & Vibration*, 329 (2010) 4515–4533.

[6] P. Warnitchai, Y. Fujino, T. Susumpow, A nonlinear dynamic model for cables and its application to a cable structure system. *Journal of Sound & Vibration*, 187(4) (1995) 695–712.

[7] D. Wagg, S. Neild, *Nonlinear Vibration with Control*, Springer, 2010.

[8] N. Srinil, G. Rega, S. Chucheepsakul, Two-to-one resonant multi-modal dynamics of horizontal/inclined cables. part i: Theoretical formulation and model validation. *Nonlinear Dynamics*, 48(3) (2007) 231–252.

[9] N. Srinil, G. Rega, Two-to-one resonant multi-modal dynamics of horizontal/inclined cables. part ii: Internal resonance activation, reduced-order models and nonlinear normal modes. *Nonlinear Dynamics*, 48(3) (2007) 253–274.

[10] E. Doedel, in *Numerical Continuation Methods for Dynamical Systems*, edited by B.Krauskopf, H. Osinga, and J. Galan-Vioque, Springer-Verlag, Dordrecht, 2007.

[11] E.J. Doedel, with major contributions from A.R. Champneys, T.F. Fairgrieve, Y.A. Kuznetsov, B. Sandstede, X.J. Wang, *AUTO2000 and AUTO-07P: Continuation and bifurcation software for ordinary differential equations*, Department of Computer Science, Concordia University, Montreal, Canada, 2000; available from `http://sourceforge.net/projects/auto2000`.

[12] J. Guckenheimer, P. Holmes. *Nonlinear Oscillations, Dynamical Systems and Bifurcations of Vector Fields*, Springer-Verlag, New York/Berlin, second edition, 1986.

[13] Y.A. Kuznetsov *Elements of Applied Bifurcation Theory*, Springer-Verlag, New York/Berlin, second edition, 1998.